

Wave-Number-Dependent Susceptibility Function for Paramagnetic Chromium<sup>†</sup>

R. P. Gupta and S. K. Sinha

*Institute for Atomic Research and Department of Physics, Iowa State University, Ames, Iowa 50010*

(Received 26 August 1970)

A detailed computation has been made of the generalized susceptibility function for paramagnetic chromium to investigate the effects of including realistic band-structure effects on both the unenhanced susceptibility and on the exchange enhancement. An augmented-plane-wave band-structure calculation for paramagnetic chromium has been performed to obtain energy bands and wave functions for the first six bands on a mesh of 1024 points in the Brillouin zone. An interpolation scheme was used to increase the effective mesh to 128 000 points in the zone and the unenhanced susceptibility function was calculated from these, both with and without the matrix elements. The matrix elements were seen to make a dramatic difference in the susceptibility, and, in fact, reduce the peak due to the "nesting" of the Fermi surface so that it is not an actual maximum of  $\chi^{(0)}(\vec{q})$ . The exchange enhancement was then investigated by approximately solving the coupled self-consistent equations for the Fourier components of the response to an applied field including local-field corrections. This yields an exchange-enhanced susceptibility function which has the tendency to first become infinite at the nesting wave vector, indicating that the local-field corrections may play an important role in determining the wave vector for instability against formation of a spin-density wave. It is also shown that the exchange-enhanced susceptibility thus obtained displays quasilocalized spin behavior of the electron response to an applied oscillatory field.

## I. INTRODUCTION

The occurrence of a spin-density wave (SDW) in chromium with a wave vector slightly incommensurate with the lattice structure has been the subject of intensive theoretical and experimental investigation over the last few years.<sup>1-12</sup> One may refer to the reviews by Herring<sup>13</sup> and Arrott<sup>14</sup> for details and a full set of references to earlier work. The instability against the formation of the SDW at a certain wave vector may be represented by the generalized susceptibility function  $\chi(\vec{q})$  in the paramagnetic phase going to infinity at that wave vector. This would, strictly speaking, result in a second-order transition to the ordered state. For pure chromium, the transition is believed to be first order.<sup>14</sup> This point is discussed more fully in Sec. IV. The divergence is caused by exchange-enhancement effects, and it is generally recognized that the shape of the Fermi surface plays a key role in choosing the SDW wave vector. This is due to the "nested" feature of the hole octahedron at *H* and electron jack at  $\Gamma$ , which are flat pieces separated by a constant wave vector  $\vec{q}_m$  which results in a peak in the unenhanced susceptibility function at that wave vector. Figure 1 illustrates this feature of the Fermi surface calculated by Loucks<sup>15</sup> for chromium. The calculations described here are in agreement with the basic features of the surface shown in Fig. 1 except that small-hole pockets at *N* are also obtained.

Detailed calculations of  $\chi(\vec{q})$  have hitherto not been made except for grossly oversimplified models of the energy-band structure of chromium, or

by neglecting completely the role of the matrix elements in the expression for the unenhanced susceptibility. The problem of accurately calculating the exchange enhancement is, however, a very difficult one, even within the spirit of the random-phase approximation. For a realistic multiband system containing Bloch electrons, one is generally forced to make both a simplification in the form of the electron-electron interaction and to make further approximations in solving the coupled set of equations describing the self-consistent linear response of the system to a weak applied field. Generally, one assumes a  $\delta$ -function-type interaction and also simply divides the unenhanced susceptibility function by a simple exchange-enhancement denominator. Recent attempts to obtain a better solution for the purposes of discussing

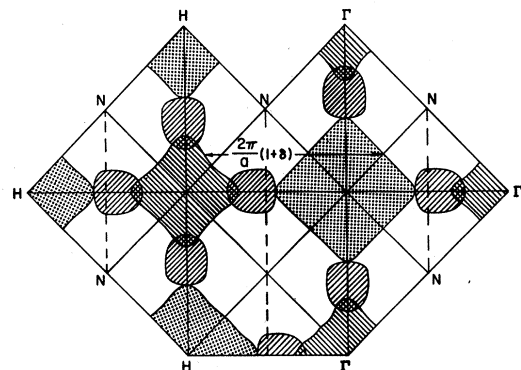


FIG. 1. Intersections of the Fermi surface of chromium with the faces of the  $\frac{1}{48}$ th zone (after Loucks).

spin waves and magnetic scattering of neutrons from itinerant electron systems have been made by Englert and Antonoff,<sup>16</sup> Yamada and Shimizu,<sup>17,18</sup> and Sokoloff.<sup>19-21</sup> These authors proceed from the Wannier representation of the electron wave functions, and a Hamiltonian similar in form to that introduced by Hubbard,<sup>22</sup> and make the simplification that some of the Bloch wave-number-dependent phase factors can be neglected in their Coulombic and exchange integrals. Thus they arrive at a result in which the exchange enhancement is taken into account by the formal inversion of a matrix involving Coulomb and exchange integrals between Wannier functions in different bands. Further approximations are then made for these integrals in order to carry out the matrix inversion, as discussed in the papers of Yamada and Shimizu.<sup>17,18</sup> These authors have not specifically applied their theory to the case of an itinerant antiferromagnet such as chromium. Sokoloff<sup>20,21</sup> has investigated the case of chromium in detail, but has used the very simplified free-electron-like band structure of the Fedders and Martin<sup>8</sup> model. Evenson *et al.*<sup>23</sup> have calculated the unenhanced susceptibility function using the energy bands of Mattheiss<sup>24</sup> for tungsten and assuming that they are similar for chromium. This function did show a peak at approximately the SDW wave vector, but in the calculation the generalized oscillator-strength matrix elements were ignored.

Here we report a multiband calculation of the unenhanced susceptibility function of paramagnetic chromium using the results of an augmented-plane-wave (APW) energy-band calculation and including the oscillator-strength matrix elements between the Bloch states. Further, we discuss an approximate solution to the exchange-enhancement problem which is similar, but not completely equivalent, to that of Yamada and Shimizu<sup>17,18</sup> and Sokoloff<sup>19-21</sup> and apply it to the case of chromium with reference to the instability against formation of the SDW. We first outline the well-established steps in setting up the expression for the exchange-enhanced susceptibility using the self-consistent field approach, which has the advantage of being conceptually simple. The same results may be derived by other methods such as the Green's-function formalisms within the random-phase approximation.

Consider the system of Bloch electrons with wave functions  $\psi_{k,\sigma}$  and energies  $E_{k,\sigma}$ , where the subscript  $k$  denotes both the Bloch wave vector and the band index and  $\sigma$  denotes the spin index. These may be taken to be the Hartree-Fock states. Now consider a weak sinusoidally varying magnetic field applied to the system, such that the perturbation may be written as

$$\mathcal{H}_1 = \sum_i g \mu_B \vec{S}_i \cdot \vec{H}_q e^{i\vec{q} \cdot \vec{r}_i}, \quad (1)$$

where  $\vec{S}_i$  is the spin of the electron  $i$ . Since we are discussing the paramagnetic case, we may, without loss of generality, take  $\vec{H}_q$  to be directed along the  $z$  axis. The total perturbation will of course include the self-consistent response of the electrons through the electron-electron interaction, which should include both Coulomb interactions leading to correlation effects of the type discussed by Hubbard<sup>22</sup> and exchange interactions. The change in the electron-electron interaction part of the effective one-electron Hamiltonian due to the self-consistent response has matrix elements between one-electron states of the form

$$\begin{aligned} \langle \psi_{k',\sigma'} | \Delta V_{\text{int}} | \psi_{k,\sigma} \rangle &= \langle \psi_{k',\sigma'} | \Delta V_{\text{HF}} | \psi_{k,\sigma} \rangle \\ &+ U \langle \psi_{k',\sigma'} | \Delta n_{d,-\sigma} | \psi_{k,\sigma} \rangle \delta_{k,d}, \end{aligned} \quad (2)$$

where  $\Delta V_{\text{HF}}$  is the change in the one-electron Hartree-Fock potential and the second term represents the linearized change in the Hubbard-type correlation interaction.  $U$  represents the strength of this interaction,  $\Delta n_{d,-\sigma}$  represents the change in the electron density of all  $d$ -like electrons with spin opposite to that of the state  $\psi_{k,\sigma}$ , and the presence of the factor  $\delta_{k,d}$  indicates that this interaction is supposed to operate only on the  $d$ -like electrons.  $\Delta V_{\text{HF}}$  has a part which depends on the total change in the electron density (Hartree part), as well as a nonlocal exchange term which depends on the change in the wave functions of states with the same spin index  $\sigma$  as the state  $\psi_{k,\sigma}$ . The first-order change in the wave function  $\Delta \psi_{k,\sigma}$  is given by first-order perturbation theory as

$$\Delta \psi_{k,\sigma} = \sum_{k',\sigma'} \frac{\langle \psi_{k',\sigma'} | \mathcal{H}_1 + \Delta V_{\text{int}} | \psi_{k,\sigma} \rangle}{E_{k,\sigma} - E_{k',\sigma'}} \psi_{k',\sigma'}. \quad (3)$$

Thus, by making Eqs. (2) and (3) self-consistent, we arrive at a set of coupled integral equations for the Fourier transform of the  $z$  component of the induced self-consistent magnetization density  $\Delta M(\vec{K})$ . As is well known,<sup>13</sup> the Hartree part of  $\Delta V_{\text{HF}}$  contributes nothing to  $\Delta M(\vec{K})$ , and we now make the usual simplification, which is still somewhat crude, of replacing the electron-electron interaction in the exchange part of  $\Delta V_{\text{HF}}$  with a  $\delta$  function  $J \delta(\vec{r} - \vec{r}')$ . Screening of the exchange due to correlation effects as well as averaging effects over the occupied electron states lends some justification for representing this as an effective short-range interaction. Further, since it is not possible to separate the  $d$ -like states from the  $s$ - and  $p$ -like states, owing to hybridization effects in transition metals, we make the further approximation of removing the  $\delta$ -function restriction on the second term of Eq. (2), i.e., we assume correlation effects between all occupied states of the system. Making these approximations, and noting that  $\Delta M(\vec{r})$  has only nonvanishing Fourier components

for  $\vec{K} = \vec{q} + \vec{G}$  where  $G$  is a reciprocal-lattice vector, one may show that the self-consistency equations for  $\Delta M(\vec{q} + \vec{G})$  are

$$\Delta M(\vec{q} + \vec{G}) = \sum_{\vec{q}'} \chi^{(0)}(\vec{q} + \vec{G}, \vec{q} + \vec{G}') \times [\delta_{0, \vec{q}} H_q + I \Delta M(\vec{q} + \vec{G}')] , \quad (4a)$$

where

$$I = -\frac{1}{2} (J + U) (2/g\mu_B)^2 , \quad (4b)$$

and  $\chi^{(0)}(\vec{q} + \vec{G}, \vec{q} + \vec{G}')$  is defined by

$$\begin{aligned} \chi^{(0)}(\vec{q} + \vec{G}, \vec{q} + \vec{G}') = & -\left(\frac{1}{2} g\mu_B\right)^2 \sum_{\vec{k}, \sigma} \frac{n_{\vec{k}, \sigma} - n_{\vec{k}', \sigma}}{E_{\vec{k}, \sigma} - E_{\vec{k}', \sigma}} \\ & \times \langle \psi_{\vec{k}, \sigma} | e^{-i(\vec{q} + \vec{G}) \cdot \vec{r}} | \psi_{\vec{k}', \sigma} \rangle \\ & \times \langle \psi_{\vec{k}', \sigma} | e^{i(\vec{q} + \vec{G}') \cdot \vec{r}} | \psi_{\vec{k}, \sigma} \rangle , \end{aligned} \quad (5)$$

where  $n_{\vec{k}, \sigma}$  refers to the occupation number of the state  $(\vec{k}, \sigma)$ . In the paramagnetic case the  $\sigma$  index may be dropped from Eq. (5) and the expression multiplied simply by a factor of 2 for spin degeneracy. The function  $\chi^{(0)}(\vec{q} + \vec{G}, \vec{q} + \vec{G}')$  is the susceptibility function which describes the  $(\vec{q} + \vec{G})$  Fourier component of the response of the noninteracting system of Bloch electrons to the  $(\vec{q} + \vec{G}')$  Fourier component of an applied field. It will depend on the energies and wave functions of the appropriate Bloch states.

The formal solution of Eq. (4) may be written in matrix form by representing the set of Fourier components  $\Delta M(\vec{q} + \vec{G})$  as a vector  $\underline{\Delta M}$ , the set of quantities  $\chi^{(0)}(\vec{q} + \vec{G}, \vec{q} + \vec{G}')$  as a matrix  $\underline{\chi}^{(0)}$ , and the quantity  $H_q$  as a one-component vector  $\underline{H}$  (only  $\vec{G} = 0$  component present), in which case (2) yields

$$\underline{\Delta M} = [1 - I \underline{\chi}^{(0)}]^{-1} \underline{\chi}^{(0)} \underline{H} , \quad (6)$$

with  $1$  denoting the unit matrix. Even within the rather crude approximation introduced above for the electron-electron interaction matrix elements, one may see that a calculation of the actual response of the system involves the nontrivial problem of inversion of the matrix  $[1 - I \underline{\chi}^{(0)}]$  which has off-diagonal elements connected by the matrix elements appearing in  $\chi^{(0)}(\vec{q} + \vec{G}, \vec{q} + \vec{G}')$  [Eq. (5)]. These off-diagonal elements will, in general, give rise to what are known as local-field corrections<sup>25-30</sup> which have hitherto been largely ignored. A common approximation is to neglect entirely the effects of the matrix elements in Eq. (5) and to write  $\chi^{(0)}$  as

$$\bar{\chi}^{(0)}(\vec{q}) = -\left(\frac{1}{2} g\mu_B\right)^2 \sum_{\vec{k}, \sigma} \frac{n_{\vec{k}} - n_{\vec{k}'}}{E_{\vec{k}} - E_{\vec{k}'}} , \quad (7)$$

where the summation again runs over a certain set of bands (to be specified below) for both states, but  $\vec{k}'$  is restricted to be the state with Bloch vector  $\vec{K}' = \vec{k} + \vec{q}$  in the reduced zone. The approximate

$\bar{\chi}^{(0)}(\vec{q})$  represented by Eq. (7) is assumed to represent the diagonal elements of  $\chi^{(0)}$ , i.e.,  $\chi^{(0)}(\vec{q}, \vec{q})$  (the off-diagonal elements being assumed to be zero) and is also periodic in reciprocal space, whereas the actual  $\chi^{(0)}(\vec{q}, \vec{q})$  is not. Furthermore, from the form of Eq. (5) it may be observed that for  $\vec{G} = \vec{G}' = 0$  and  $\vec{q} = 0$  the interband matrix elements vanish while the intraband matrix elements tend to unity resulting in  $\chi^{(0)}(\vec{q}, \vec{q})$  tending to  $(\frac{1}{2} g\mu_B)^2 N(E_F) \times (\vec{q} \rightarrow 0)$  where  $N(E_F)$  is the density of states at the Fermi level. Since the matrix elements are ignored in Eq. (7),  $\bar{\chi}^{(0)}(\vec{q})$  will deviate considerably from the correct value at  $\vec{q} = 0$  unless there is only one band at the Fermi level and the expression in Eq. (7) involves only that band. However, in that case, the neglect of the interband matrix elements will lead to errors at finite  $\vec{q}$ .

However, if one makes the above approximations, one obtains from Eq. (6)

$$\Delta M(\vec{q}) = \frac{\bar{\chi}^{(0)}(\vec{q})}{1 - I \bar{\chi}^{(0)}(\vec{q})} H_q , \quad (8)$$

or equivalently

$$\chi(\vec{q}) = \frac{\bar{\chi}^{(0)}(\vec{q})}{1 - I \bar{\chi}^{(0)}(\vec{q})} , \quad (9)$$

which is the commonly assumed form for the exchange-enhanced susceptibility  $\chi(\vec{q})$ . It should be noticed that Eqs. (7)–(9) are only strictly correct for free electrons [if Eq. (5) is to be interpreted according to the selection rule  $\vec{K}' = \vec{k} + \vec{q}$  in the extended zone scheme]. However, for the reasons mentioned above these expressions may be completely unrealistic for the Bloch states of a transition metal.

Accordingly, we will first discuss an attempt at a more realistic calculation of the diagonal elements  $\chi^{(0)}(\vec{q}, \vec{q})$  [henceforth referred to simply as  $\chi^{(0)}(\vec{q})$ ] from Eq. (5) using the result of an actual APW band calculation for paramagnetic chromium, and later an approximation for obtaining the solution to Eq. (6) which involves not only such diagonal elements but which also approximately takes into account the effect of the off-diagonal elements  $\chi^{(0)}(\vec{q} + \vec{G}, \vec{q} + \vec{G}')$ .

## II. PARAMAGNETIC BAND STRUCTURE OF CHROMIUM

The starting point for the calculation of  $\chi^{(0)}(\vec{q})$  is the availability of realistic and accurate energy bands and wave functions for a large number of points in the Brillouin zone. There have been several studies of the electronic structure of chromium, but the authors have mostly confined themselves to an investigation of the Fermi surface only. Lomer<sup>31</sup> was the first to propose a model of the Fermi surface of chromium. This was not based on an *ab initio* calculation but was deduced from the energy bands of iron calculated by Wood by the APW method

and also the tight-binding calculation of Asdente and Friedel.<sup>32</sup> A few years later, Loucks<sup>15</sup> calculated the muffin-tin potential for chromium which he then used to determine the Fermi surface. His results confirmed the model of the Fermi surface of chromium proposed by Lomer. In Loucks's calculation, the APW method was used and the wave function was expanded in a basis set of 19 reciprocal-lattice vectors. More recently, Asano and Yamashita<sup>12</sup> did a band calculation for chromium both in the paramagnetic and the antiferromagnetic phase using the Korringa-Kohn-Rostoker (KKR) method. Their results also supported the conclusions of Lomer. Besides the Fermi surface they also calculated the energy bands in symmetry directions.

In the present work, we have calculated the energy bands of chromium by the APW method. In this calculation, a muffin-tin version of the crystal potential was used. The atomic-charge densities of Liberman *et al.*<sup>33</sup> from self-consistent field atomic calculations were used to construct the crystal potential in the manner suggested by Mattheis.<sup>24</sup> The contribution of exchange was included using Slater's  $\rho^{1/3}$  approximation. A basis set of 43 reciprocal-lattice vectors was chosen to expand the wave function. These reciprocal-lattice vectors are listed in Table I in the notation  $(lmn) = (2\pi/a)(l\hat{i} + m\hat{j} + n\hat{k})$ , where  $\hat{i}, \hat{j}, \hat{k}$  are the unit vectors along the three Cartesian axes. The energy eigenvalues were converged to within 0.001 Ry at the symmetry points using this set of reciprocal-lattice vectors. A mesh of 1024 points in the whole Brillouin zone was chosen for the purpose of calculation. By taking symmetry considerations into account, however, the actual calculations were performed for only 55 points lying in the  $\frac{1}{48}$ th of the Brillouin zone which is irreducible under symmetry operations. The first six bands for all the

55 points are given in Table II. These bands are shown along the symmetry direction in Fig. 2. The APW expansion coefficients of the wave functions were obtained by the Jacobi method of diagonalizing the matrix. The energy bands so calculated seem to be in reasonable agreement with recent data on optical transitions in chromium obtained by Bos and Lynch.<sup>34</sup>

To obtain the density of states and the Fermi energy reasonably accurately, the mesh in the Brillouin zone was expanded to a total of 128 000 points and the energy bands in the expanded mesh were obtained by the method of "spline interpolation."<sup>35</sup> The spline interpolation is essentially a third-degree polynomial interpolation in which the curve connecting the points, its slope, and its curvature are all kept continuous everywhere. For the sake of clarity, the method is briefly described below. Let us assume that we have an ordered linear array of  $n$  points  $x_1, x_2, \dots, x_n$ . Also suppose that the function has the values  $y_1, y_2, \dots, y_n$  at these points and its second derivatives are  $g_1, g_2, \dots, g_n$ . By linear interpolation, the second derivative at the point  $x$  lying between  $x_m$  and  $x_{m+1}$  is given by

$$y'' = g_m + (g_{m+1} - g_m)(x - x_m)/h_m, \quad (10)$$

where  $h_m = x_{m+1} - x_m$ . On integration, the equation of the curve between  $x_m$  and  $x_{m+1}$  is found to be

$$y = (x_{m+1} - x)^3 \frac{g_m}{6h_m} + (x - x_m)^3 \frac{g_{m+1}}{6h_m} + (x_{m+1} - x) \left( \frac{y_m}{h_m} - \frac{g_m h_m}{6} \right) + (x - x_m) \left( \frac{y_{m+1}}{h_m} - \frac{g_{m+1} h_m}{6} \right). \quad (11)$$

The only unknown quantities in this equation are the second derivatives  $g_m$  and  $g_{m+1}$ . These are determined by solving a set of  $n$  linear equations. One makes use of the fact that the slope of the curve at the point  $x_m$  determined from the equation involving the set of points  $(x_{m-1}, x_m)$  is identical to the one from  $(x_m, x_{m+1})$ . The following relation is then obtained:

$$\frac{1}{6} g_{m-1} h_{m-1} + \frac{1}{3} g_m (h_{m-1} + h_m) + \frac{1}{6} g_{m+1} h_m = \frac{y_{m+1} - y_m}{h_m} - \frac{y_m - y_{m-1}}{h_{m-1}}. \quad (12)$$

Such an equation is obtained for each point on the curve except the end points. Thus, we have a set of  $(n-2)$  linear equations containing  $n$  unknown constants. By specifying two appropriate boundary conditions, the  $g_m$ 's are determined and hence the interpolation carried out.

The density-of-states curve calculated in this way using a mesh of 128 000 points in the Brillouin zone is shown in Fig. 3. The Fermi energy occurs

TABLE I. Reciprocal-lattice vectors used in APW expansion for all points in the zone. They are listed in order of importance for the zone as a whole (based on  $\vec{k}_i = \vec{k} + \vec{g}_i$ ).

( 0 0 0)	(-1 -1 0)	( 0 -1 -1)
(-1 0 -1)	(-2 0 0)	(-1 1 0)
(-1 0 1)	( 0 -1 1)	( 1 0 -1)
( 1 -1 0)	( 0 1 -1)	( 1 1 0)
( 1 0 1)	( 0 1 1)	( 0 -2 0)
(-1 -1 -2)	(-1 -2 -1)	(-2 -1 -1)
( 0 0 -2)	(-2 1 -1)	(-2 -1 1)
(-2 1 1)	(-1 -2 1)	( 2 0 0)
( 0 2 0)	( 0 0 2)	(-2 -2 0)
(-1 -1 2)	( 1 -1 -2)	( 1 -2 -1)
(-1 1 -2)	( 0 -2 -2)	(-2 0 -2)
(-3 0 -1)	(-1 2 -1)	(-3 -1 0)
(-3 1 0)	(-2 2 0)	(-3 0 1)
(-1 2 1)	(-2 0 2)	(-1 1 2)
( 1 -2 1)		

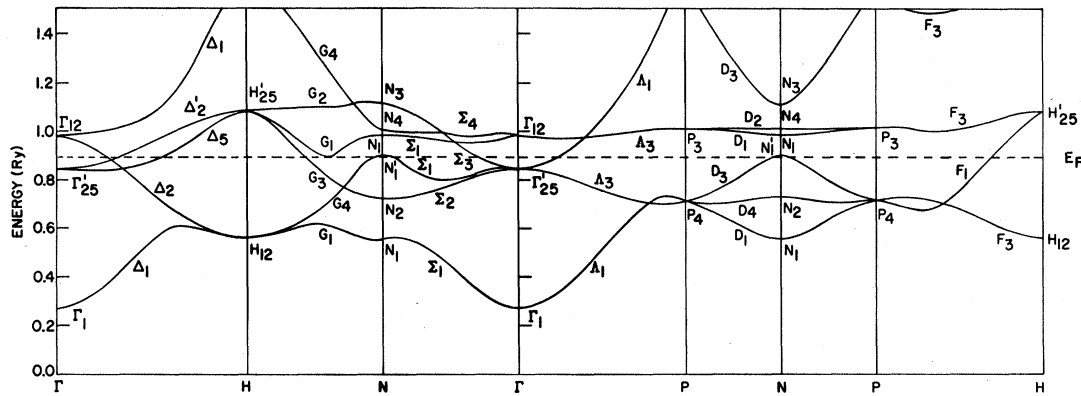


FIG. 2. Energy bands of chromium along symmetry directions.

at 0.896 Ry, and the density of states at this value of energy is found to be 7.36 states/Ry atom which is in good agreement with the value 7.10 states/Ry atom obtained earlier by Loucks in his APW calculation. It is to be noted that experimental electronic specific-heat data<sup>36</sup> for chromium indicate an electron-phonon mass-enhancement factor of about 20% based on the above density of states (assuming the latter does not change very much in the transition to the ordered state). This value is consistent also with the estimates of Rice *et al.*<sup>37</sup> for the mass enhancement in chromium.

### III. CALCULATION OF UNENHANCED SUSCEPTIBILITY

The unenhanced generalized susceptibility function  $\bar{\chi}^{(0)}(\vec{q})$  calculated without matrix elements, i.e., using the approximation in Eq. (7) and summing over all six bands, with an expanded mesh of 128 000 points in the Brillouin zone, is shown in Fig. 4. It is basically similar to that obtained by Evenson *et al.*<sup>23</sup> who, however, used a considerably smaller mesh. The function  $\bar{\chi}^{(0)}(\vec{q})$  shows a peak at  $(2\pi/a)(0.88, 0, 0)$ . One notices that the value at  $\vec{q} = (0, 0, 0)$  is not equal to  $(\frac{1}{2}g\mu_B)^2 N(E_F)$  and, in fact, differs from it by a factor of 20. This is due to the neglect of the matrix elements as discussed in Sec. I.

In order to examine the difference which the matrix elements make,  $\chi^{(0)}(\vec{q})$  was calculated including matrix elements with a small mesh of 1024 points in the zone. The method for calculating the matrix elements is described in the Appendix. The resulting curve is shown in Fig. 5 where the contributions from intraband and interband matrix elements are also shown. We notice that the inclusion of the matrix elements has a drastic effect on both the magnitude of  $\chi^{(0)}(\vec{q})$  and on the shape of the curve. It must be realized, as pointed out by Evenson and Liu,<sup>38</sup> that the results for  $\chi^{(0)}(\vec{q})$  obtained using a mesh as small as 1024 points in the entire Brillouin zone may be unreliable. The

calculation was therefore repeated with a finer mesh of 128 000 points. The calculation of matrix elements for such a large mesh requires a prohibitively large amount of machine time. However, we may assume that these matrix elements vary very slowly with  $\vec{q}$ . The matrix elements calculated for the coarser mesh of 1024 points for all the  $\vec{q}$  vectors of interest commensurate with this mesh were therefore stored on magnetic tape. For every set of Bloch wave vectors  $\vec{k}, \vec{k}'$  in the finer mesh the energy denominators used in Eq. (5) were obtained using the interpolation scheme described in Sec. II, but the matrix elements were used between states  $\vec{k}, \vec{k}'$  which lay on the coarser mesh closest to  $\vec{k}, \vec{k}'$ , respectively. The resulting  $\chi^{(0)}(\vec{q})$

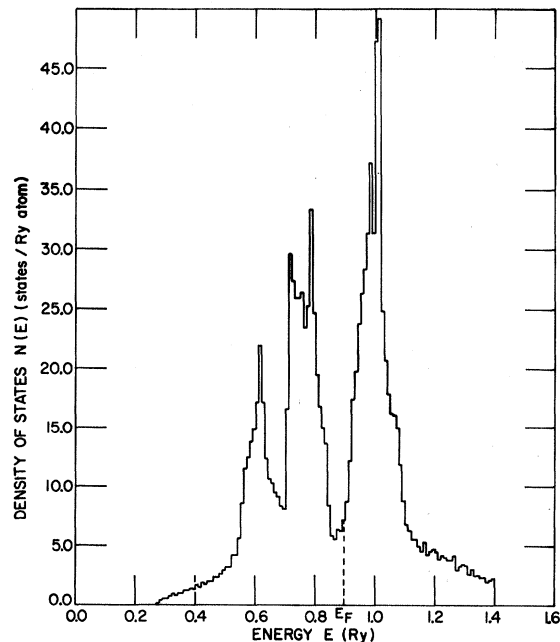


FIG. 3. Density-of-states histogram for chromium using a mesh of 128 000 points in the Brillouin zone.

for  $\vec{q}$  along the [100] direction is shown in Fig. 6. Comparison with Fig. 5 shows that the increase in the mesh size affects the  $\chi^{(0)}(\vec{q})$  in two respects. In the first place, the shape of the curve is changed

in the first zone, and secondly, the magnitude of  $\chi^{(0)}(\vec{q})$  undergoes an over-all increase in the first two zones. One also notices that the results from the two calculations are closer for larger  $\vec{q}$  values.

TABLE II. Energy bands of chromium.

	$(4a/\pi) \vec{k}$	Band 1	Band 2	Band 3	Band 4	Band 5	Band 6
$\Gamma$	(0 0 0)	0.272	0.845	0.845	0.845	0.981	0.981
	(1 0 0)	0.296	0.843	0.843	0.853	0.961	0.987
	(2 0 0)	0.363	0.841	0.841	0.876	0.908	1.005
	(3 0 0)	0.460	0.832	0.848	0.848	0.913	1.031
	(4 0 0)	0.555	0.750	0.873	0.873	0.957	1.072
	(5 0 0)	0.606	0.673	0.919	0.919	1.004	1.162
	(6 0 0)	0.599	0.612	0.983	0.983	1.045	1.317
$H$	(7 0 0)	0.572	0.573	1.050	1.050	1.073	1.499
	(8 0 0)	0.560	0.560	1.083	1.083	1.083	1.602
	(1 1 0)	0.319	0.825	0.837	0.877	0.962	0.981
	(2 1 0)	0.384	0.812	0.823	0.912	0.930	0.998
	(3 1 0)	0.475	0.796	0.812	0.898	0.954	1.026
	(4 1 0)	0.565	0.741	0.832	0.897	1.000	1.074
	(5 1 0)	0.614	0.677	0.873	0.916	1.044	1.180
	(6 1 0)	0.609	0.623	0.934	0.959	1.077	1.346
	(7 1 0)	0.584	0.587	1.003	1.019	1.088	1.515
	(2 2 0)	0.439	0.781	0.801	0.958	0.963	0.988
	(3 2 0)	0.510	0.768	0.788	0.951	1.011	1.013
	(4 2 0)	0.571	0.762	0.777	0.940	1.058	1.072
	(5 2 0)	0.609	0.716	0.810	0.921	1.089	1.199
	(6 2 0)	0.619	0.664	0.866	0.925	1.098	1.339
$N$	(3 3 0)	0.540	0.741	0.823	0.979	1.001	1.065
	(4 3 0)	0.562	0.739	0.837	0.972	1.046	1.099
	(5 3 0)	0.585	0.763	0.784	0.945	1.109	1.148
	(4 4 0)	0.556	0.726	0.899	0.984	1.008	1.114
	(1 1 1)	0.342	0.818	0.818	0.901	0.971	0.971
	(2 1 1)	0.404	0.800	0.801	0.942	0.944	0.993
	(3 1 1)	0.492	0.772	0.800	0.915	0.987	1.024
	(4 1 1)	0.577	0.729	0.816	0.910	1.016	1.090
	(5 1 1)	0.628	0.677	0.834	0.938	1.042	1.210
	(6 1 1)	0.625	0.629	0.874	0.992	1.062	1.382
	(7 1 1)	0.598	0.598	0.941	1.055	1.055	1.565
	(2 2 1)	0.460	0.772	0.780	0.964	0.987	0.995
	(3 2 1)	0.530	0.752	0.774	0.955	1.007	1.053
	(4 2 1)	0.590	0.734	0.781	0.947	1.030	1.130
	(5 2 1)	0.629	0.709	0.785	0.947	1.056	1.252
	(6 2 1)	0.637	0.668	0.812	0.970	1.065	1.391
	(3 3 1)	0.562	0.734	0.795	0.980	1.002	1.107
	(4 3 1)	0.582	0.731	0.815	0.977	1.024	1.162
	(5 3 1)	0.604	0.747	0.775	0.960	1.056	1.230
	(4 4 1)	0.576	0.720	0.860	0.988	1.009	1.171
	(2 2 2)	0.514	0.751	0.751	0.983	0.983	1.056
	(3 2 2)	0.579	0.728	0.747	0.974	1.004	1.122
	(4 2 2)	0.628	0.709	0.763	0.968	1.018	1.205
	(5 2 2)	0.670	0.694	0.751	0.978	1.025	1.333
	(6 2 2)	0.680	0.680	0.748	1.012	1.012	1.498
	(3 3 2)	0.619	0.720	0.744	0.991	1.004	1.191
	(4 3 2)	0.633	0.714	0.770	0.990	1.014	1.266
	(5 3 2)	0.652	0.720	0.751	0.986	1.020	1.349
	(4 4 2)	0.628	0.710	0.795	0.998	1.011	1.290
	(3 3 3)	0.685	0.709	0.709	1.005	1.005	1.279
	(4 3 3)	0.679	0.710	0.737	1.004	1.011	1.370
	(5 3 3)	0.678	0.725	0.725	1.006	1.006	1.483
	(4 4 3)	0.687	0.704	0.744	1.009	1.013	1.432
$P$	(4 4 4)	0.714	0.714	0.714	1.014	1.014	1.583

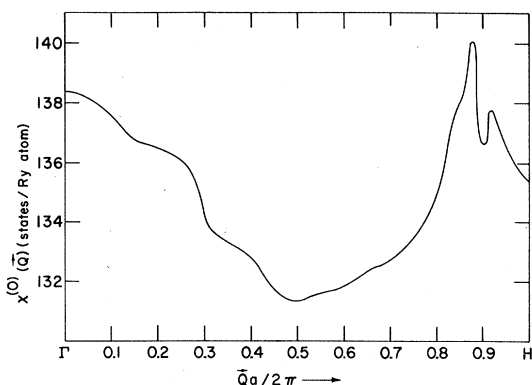


FIG. 4. The unenhanced susceptibility function  $\bar{\chi}^{(0)}(\vec{q})$  in units of  $(\frac{1}{2}g\mu_B)^2$  calculated using a mesh of 128 000 points in the Brillouin zone and ignoring the matrix elements ( $T=0$ ).

Notice in Fig. 6 that  $\chi^{(0)}(\vec{q})$  approaches the correct value of  $(\frac{1}{2}g\mu_B)^2 N(E_F)$  at  $\vec{q}=0$ , as expected, and shows a peak at the nesting wave vector. Contrary to expectations, however, a broad maximum at a  $\vec{q}$  other than the nesting  $\vec{q}$  is also obtained. This is presumably due to the suppression of the peak at the nesting wave vector near the zone boundary due to the matrix elements, and also the drastic suppression of the interband matrix elements near  $\vec{q}=0$ . As may be seen from Fig. 5, both intra- and interband contributions show the correct qualitative behavior, namely, the intraband contribution drops off rapidly with increasing  $\vec{q}$ , and it is only the interband contribution which is important for larger  $\vec{q}$  values. It is to be noted that the peak at the nesting wave vector itself arises from purely interband transitions, both the bands concerned lying close to the Fermi level. We have previously<sup>39</sup> calculated the  $\chi^{(0)}(\vec{q})$  in a similar manner by extending the plane-wave components of the wave function outside the APW sphere over the entire cell and suitably renormalizing the wave function. There, also, a peak at the nesting wave vector and a higher and much broader peak elsewhere were obtained. A comparison with present results seems to indicate that the earlier approximation overestimates the magnitude of  $\chi(\vec{q})$  but does not alter most of the conclusions drawn from that calculation.

The above calculations were performed for occupation numbers appropriate to  $T=0$ . The same calculation was repeated for  $T=T_N$  to examine the temperature dependence of the function  $\chi^{(0)}(\vec{q})$  by inserting in Eq. (5) the actual Fermi-Dirac occupation numbers for that temperature. A significant change in the function could not be found. The apparent decrease on increasing temperature found previously<sup>39</sup> has been traced to a minor computational error in the earlier calculation.

In order to explain the appearance of the SDW into the observed wave vector, we have to examine the solutions to Eq. (4) more carefully.

#### IV. EXCHANGE-ENHANCED SUSCEPTIBILITY

We may write

$$\chi^{(0)}(\vec{q}+\vec{G}, \vec{q}+\vec{G}') = \chi_{\text{inter}}^{(0)}(\vec{q}+\vec{G}, \vec{q}+\vec{G}') + \chi_{\text{intra}}^{(0)}(\vec{q}+\vec{G}, \vec{q}+\vec{G}'), \quad (13)$$

where the terms on the right-hand side represent, respectively, the contributions of the interband and intraband matrix elements. We then make the ansatz that the first term may be written as

$$\chi_{\text{inter}}^{(0)}(\vec{q}+\vec{G}, \vec{q}+\vec{G}') = f(\vec{q}+\vec{G})f^*(\vec{q}+\vec{G}')\bar{\chi}^{(0)}(\vec{q}), \quad (14)$$

where  $\bar{\chi}^{(0)}(\vec{q})$  is defined by Eq. (7) where the sum is now to be taken over all interband transitions only, and  $f(\vec{q}+\vec{G})$  is an averaged generalized oscillator-strength matrix element

$$\langle \Psi_k | e^{-i(\vec{q}+\vec{G}) \cdot \vec{r}} | \Psi_{k'} \rangle,$$

for all such transitions. It is obvious that Eq. (14) is not a valid approximation for the second term, since for small  $(\vec{q}+\vec{G})$  at least, the second term tends to become diagonal in  $\vec{G}, \vec{G}'$ . However, we further note that at the wave vectors of interest [i.e.,  $(\vec{q}_m+\vec{G})$  where  $\vec{q}_m = (2\pi/a)(0.88, 0, 0)$ ] the previous calculations showed that the contributions of the intraband matrix elements to  $\chi^{(0)}(\vec{q}+\vec{G}, \vec{q}+\vec{G}')$  were negligible compared to the interband contributions. Hence, in our further discussion, we may neglect the second term entirely and write

$$\chi^{(0)}(\vec{q}+\vec{G}, \vec{q}+\vec{G}') \approx f(\vec{q}+\vec{G})f^*(\vec{q}+\vec{G}')\bar{\chi}^{(0)}(\vec{q}). \quad (15)$$

Now we may obtain a solution to Eqs. (4) by writing

$$\Delta M(\vec{q}+\vec{G}) = f(\vec{q}+\vec{G})w_q. \quad (16)$$

Substituting (15) and (16) in Eq. (4), we obtain a single equation for  $w_q$  which yields the solution

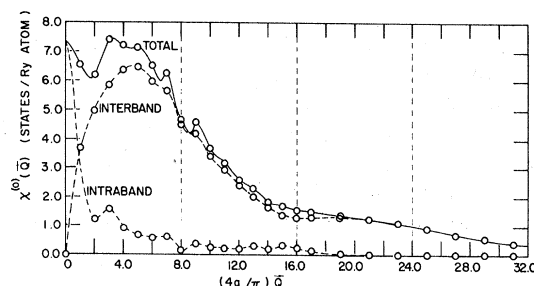


FIG. 5. The unenhanced susceptibility function  $\chi^{(0)}(\vec{q})$  in units of  $(\frac{1}{2}g\mu_B)^2$  calculated using a mesh of 1024 points in the Brillouin zone ( $T=0$ ). The contributions involving intra- and interband matrix elements are individually indicated by dashed curves.

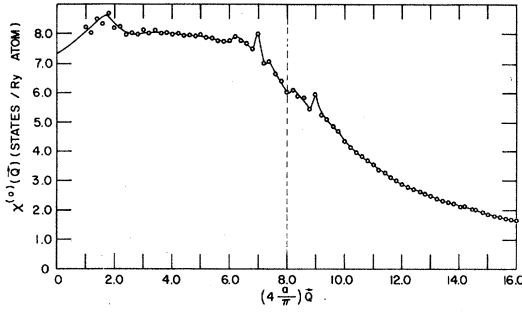


FIG. 6. The unenhanced susceptibility function  $\chi^{(0)}(\vec{q})$  in units of  $(\frac{1}{2}g\mu_B)^2$  calculated using a mesh of 128 000 points in the Brillouin zone ( $T=0$ ).

$$w_a = \frac{\bar{\chi}^{(0)}(\vec{q}) f^*(\vec{q}) H_a}{1 - I \sum_{\vec{G}} f(\vec{q} + \vec{G}) f^*(\vec{q} + \vec{G}') \bar{\chi}^{(0)}(\vec{q})} \quad (17)$$

Using Eqs. (15) and (16) we finally obtain for the diagonal element of the exchange-enhanced susceptibility in the approximation

$$\chi(\vec{q}, \vec{q}) = \chi^{(0)}(\vec{q}, \vec{q}) / [1 - I \sum_{\vec{G}} \chi^{(0)}(\vec{q} + \vec{G}', \vec{q} + \vec{G}')]. \quad (18)$$

Note that the local-field corrections have resulted in  $\sum_{\vec{G}} \chi^{(0)}(\vec{q} + \vec{G}', \vec{q} + \vec{G}')$  entering the denominator in place of the usual  $\chi^{(0)}(\vec{q}, \vec{q})$  [cf. Eq. (9)]. Thus, the denominator will first vanish where  $\sum_{\vec{G}} \chi^{(0)}(\vec{q} + \vec{G}', \vec{q} + \vec{G}')$  has its maximum rather than where  $\chi^{(0)}(\vec{q}, \vec{q})$  possesses its maximum. It is to be noted from Fig. 5 that if we represent the position of the peak in  $\chi^{(0)}(\vec{q}, \vec{q})$  at  $(2\pi/a)(0.88, 0, 0)$  as  $(2\pi/a) \times (1 - \delta, 0, 0)$ , there will also be nesting (although with different matrix elements) at  $(2\pi/a)(1 + \delta, 0, 0)$  resulting in another peak which, however, will be much smaller. These two peaks combine in the sum  $\sum_{\vec{G}} \chi^{(0)}(\vec{q} + \vec{G}', \vec{q} + \vec{G}')$ , whereas the first broad peak in  $\chi^{(0)}(\vec{q}, \vec{q})$  combines with much smaller values when a reciprocal-lattice vector is added to the appropriate wave vector. Thus, the peak due to the nesting is likely to be favored in such an expression over the other peak. Figure 7 shows the function  $\sum_{\vec{G}} \chi^{(0)}(\vec{q} + \vec{G}', \vec{q} + \vec{G}')$  for  $\vec{q}$  along the [100] direction calculated including a sum over all the first 49 reciprocal-lattice vectors closest to the origin. We have assumed that  $\chi^{(0)}(\vec{q}, \vec{q})$  is isotropic with respect to the direction of  $\vec{q}$ . It may be seen that in this sum, the peak at  $(2\pi/a)(0.88, 0, 0)$  is indeed the absolute maximum. Note that the function is now periodic in the reciprocal lattice so that it has only to be calculated in the first zone. Thus, the denominator will first vanish for  $\vec{q} = (2\pi/a) \times (0.88, 0, 0)$ . This compares quite well with the experimental value of  $\vec{q} = (2\pi/a)(0.952, 0, 0)$  at  $T_N$  obtained by neutron diffraction.<sup>4</sup> The relatively coarse mesh of  $\vec{k}$  points used in our calculations, together with other approximations introduced,

including the potential used for the energy-band calculation and the simplification introduced for the electron-electron interaction are such as to preclude an accurate determination of the exact value of the wave vector at which  $\chi(\vec{q}, \vec{q})$  first becomes infinite.

It would thus appear from the above calculations that the Fermi-surface nesting alone is not enough to cause the SDW to choose the observed wave vector, if allowance is made for the matrix elements. The local-field corrections when approximately taken into account in our model for the exchange-enhanced susceptibility result, however, in the denominator of the exchange-enhanced susceptibility being replaced by  $[1 - I \sum_{\vec{G}} \chi^{(0)}(\vec{q} + \vec{G}', \vec{q} + \vec{G}')] rather than  $[1 - I \chi^{(0)}(\vec{q}, \vec{q})]$  as in the case where these corrections are ignored. Thus it would appear that these local-field corrections play an important role in determining the wave vector chosen by the SDW. Further, it may be seen from the above considerations that local-field corrections actually help the system to go unstable, in other words, they dramatically increase the exchange enhancement.$

It is almost certainly true that our approximation has, in fact, overestimated the exchange enhancement. For instance, a better approximation would have been to replace the electron-electron interaction parameter  $I$  by some  $\vec{q}$ -dependent function  $I(\vec{q})$  which would be rapidly damped out at larger values of  $\vec{q}$ . In that case, the solution given in Eq. (18) for the exchange enhancement would have to be replaced by

$$\chi(\vec{q}, \vec{q}) = \chi^{(0)}(\vec{q}, \vec{q}) / [1 - \sum_{\vec{G}} I(\vec{q} + \vec{G}') \chi^{(0)}(\vec{q} + \vec{G}', \vec{q} + \vec{G}')]. \quad (19)$$

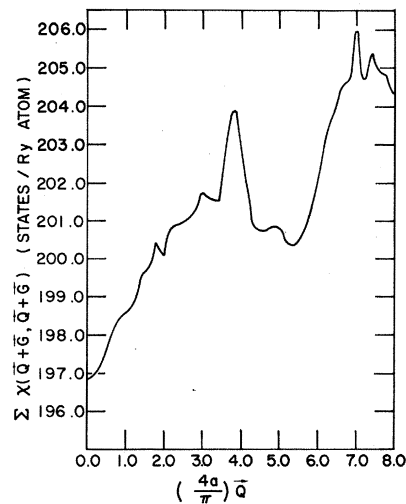


FIG. 7. The function  $\sum_{\vec{G}} \chi^{(0)}(\vec{q} + \vec{G}', \vec{q} + \vec{G}')$  in units of states/Ry atom.



The denominator in Eq. (19) would only be zero for values of the electron-electron interaction larger than that given in Eq. (18). Further, the approximation represented in Eq. (14) probably overestimates the effect of the local-field corrections, just as the conventional approximation in Eq. (9) underestimates them. It is to be noted that the experimental data<sup>6</sup> indicate that for pure and strain-free single crystals of chromium, the actual transition to the SDW state is, in fact, first order. Thus, strictly speaking, before the exchange-enhanced susceptibility goes to infinity (which would yield a second-order phase transition), the difference in *free energies* between the paramagnetic and SDW states must vanish. However, it must also be true that the vanishing of the free-energy difference will be anticipated by a sharp rise in  $\chi(\vec{q}, \vec{q})$  at the SDW wave vector, as indicated by the theory given above, even though the theory probably breaks down very close to the transition. The difference in free energies between the paramagnetic and SDW phases has been calculated by Kimball and Falicov,<sup>10</sup> by Kimball,<sup>11</sup> by Asano and Yamashita,<sup>12</sup> and by Shibatani *et al.*<sup>9</sup> They variously estimate the minimum electron-electron interaction energy required for stability of the SDW phase to be  $\sim 0.5$ – $1.5$  eV. The free-energy calculations of these authors are based essentially on the Hartree-Fock calculation of the energy of the paramagnetic state. Thus, the tendency towards SDW ordering which already exists in the paramagnetic phase, as represented by our exchange-enhancement calculation in the random-phase approximation, is ignored in these calculations and this may decrease the electron-electron interaction required. We should bear in mind that the interaction  $I$  is in any case decreased considerably by screening and phonon effects.<sup>13,40</sup> To summarize, the main conclusions of the present calculation are that (i) the matrix elements make a drastic difference in both the magnitude and the form of the function  $\chi^{(0)}(\vec{q})$ , the unenhanced susceptibility, (ii) the local-field corrections, representing the off-diagonal elements of  $\chi^{(0)}(\vec{q} + \vec{G}, \vec{q} + \vec{G}')$  play an important role in the exchange enhancements. These are probably responsible for the choice of the wave vector of the SDW and work towards increasing the tendency towards the ordered phase more than the conventional approximations for this exchange enhancement indicate, and (iii) our way of taking these into account probably overestimates the exchange-enhancement effect, and since our calculations are not valid except in the paramagnetic phase they are probably not valid very close to the phase transition, which is first order.

Finally, we close with a discussion of the nature of the solution for the exchange-enhanced suscep-

tibility as given by Eq. (19). Combining Eqs. (14) and (19) we may write

$$1 - \sum_{\vec{G}} I(\vec{q} + \vec{G}') \chi^{(0)}(\vec{q} + \vec{G}', \vec{q} + \vec{G}') \\ = 1 - \bar{\chi}^{(0)}(\vec{q}) \sum_{\vec{G}} I(\vec{q} + \vec{G}') f(\vec{q} + \vec{G}') f^*(\vec{q} + \vec{G}'). \quad (20)$$

The sum over  $\vec{G}'$  on the right-hand side of Eq. (20) is obviously periodic in the space of the reciprocal lattice, and may be written as

$$\sum_{\vec{G}'} I(\vec{q} + \vec{G}') f(\vec{q} + \vec{G}') f^*(\vec{q} + \vec{G}') = \frac{1}{N} \sum_{ij} J_{ij} e^{i\vec{q} \cdot \vec{R}_{ij}}, \quad (21)$$

where  $N$  is the total number of atoms in the crystal,  $i, j$  run over lattice sites,  $\vec{R}_{ij}$  is the separation between these sites, and  $J_{ij}$  is a generalized exchange integral representing the interaction of two spin distributions with form factors  $f(\vec{K})$  centered on the sites  $i, j$  and interacting via an effective interaction whose transform is  $I(\vec{K})$ .

Thus, Eq. (19) yields, using Eqs. (14), (20), and (21),

$$\chi(\vec{q}, \vec{q}) = f^2(\vec{q}) \bar{\chi}^{(0)}(\vec{q}) / \left( 1 - \frac{2}{N} \bar{\chi}^{(0)}(\vec{q}) \sum_{ij} \frac{1}{2} J_{ij} e^{i\vec{q} \cdot \vec{R}_{ij}} \right). \quad (22)$$

This shows that the  $q$ -dependent susceptibility of the system behaves very much like that of a localized Heisenberg system within the equivalent (random-phase) approximation, as may be seen by comparing Eq. (22) with  $\chi(\vec{q})$  obtained for the latter type of system by Liu,<sup>41</sup> and Kawasaki and Mori.<sup>42</sup> On the other hand, the expression obtained in the usual random-phase treatment, neglecting the local-field corrections [Eq. (9)], does not have a denominator which is periodic in reciprocal space. This is understandable because our assumption for the form of  $\chi^{(0)}(\vec{q} + \vec{G}, \vec{q} + \vec{G}')$  as given in Eq. (14) already has built into it the localized nature of the electronic response. This may be seen by noticing that Eq. (22) is equivalent to writing the induced magnetization as

$$\Delta M(\vec{q} + \vec{G}) = \frac{f(\vec{q} + \vec{G}) \bar{\chi}^{(0)}(\vec{q}) [f^*(\vec{q}) H_q]}{1 - (2/N) \bar{\chi}^{(0)}(\vec{q}) \sum_{ij} \frac{1}{2} J_{ij} e^{i\vec{q} \cdot \vec{R}_{ij}}} \quad (23)$$

which corresponds to an induced localized moment distribution on each site possessing a form factor  $f(\vec{K})$  and responding with a susceptibility

$$\bar{\chi}^{(0)}(\vec{q}) / \left( 1 - \frac{2}{N} \bar{\chi}^{(0)}(\vec{q}) \sum_{ij} \frac{1}{2} J_{ij} e^{i\vec{q} \cdot \vec{R}_{ij}} \right)$$

to the field *averaged* over this distribution as represented by the factor  $[f^*(\vec{q}) H_q]$ . In fact, there is a close analogy between the situation here and that pertaining to the dielectric response of the electrons in an insulator to an applied *electrostatic* potential  $v(r) = e V_q e^{i\vec{q} \cdot \vec{r}}$ .

It is well known<sup>43</sup> that the self-consistent induced

charge density is given in terms of its Fourier components by

$$\Delta\rho = \sum_{\vec{q}} [1 - v_q \chi^{(0)}]^{-1} \chi^{(0)} V, \quad (24)$$

where  $\chi^{(0)}$  now stands for the matrix  $\chi^{(0)}(\vec{q} + \vec{G}, \vec{q} + \vec{G}')$ , but with  $(\frac{1}{2}g\mu_B)^2$  in Eq. (5) replaced by  $(-e^2)$ , and  $\Delta\rho$  stands for the set of components  $\Delta\rho(\vec{q} + \vec{G})$ , while  $V$  stands for the component vector  $V_q$ . The  $v_q$  is now  $[I(\frac{1}{2}g\mu_B)^2 + 4\pi e^2/q^2]$ , i. e., the total electron-electron interaction including the Hartree term. Equation (24) is to be compared with Eq. (6). One has the same problem of formally inverting the matrix  $[1 - v_q \chi^{(0)}]$  for a solid with wave functions which are not plane waves. For an insulator, it has been shown by one of the authors<sup>44</sup> and by others<sup>30</sup> that in this case an assumption very similar to that made in Eq. (14) yields a dipolar model for the response function, i. e., describes the induced charge density in terms of dipolar distributions with form factors  $f(\vec{K})$  centered on the lattice sites. This approach can be used to derive the so-called "shell model" of lattice dynamics<sup>45</sup> (which is essentially a localized dipolar model) from the general formulation in terms of Bloch states. In both the electrostatic and magnetic cases, the localized or itinerant nature of the response to an applied disturbance will depend on the best guess as to the nature of the solutions to the self-consistent field equations of the type of Eq. (4). Such a guess will depend partly on anticipating the physical nature of the response, and the approximations introduced [as in Eq. (14)] hopefully should be consistent with such a consideration. The analogy here with the dipolar insulator just discussed is based on the fact that in both cases *interband* matrix elements probably dominate the expression in Eq. (5). In the magnetic case, of course, further localization of the response may arise from a more accurate treatment of the Hund's-rule-type correlations, and, in fact, such local moments may spontaneously exist (as in iron or cobalt). The conditions for the latter case have been discussed by several authors.<sup>13,22,46</sup> In the case of chromium, the absence of diffuse elastic scattering of neutrons in the paramagnetic phase<sup>47</sup> and other evidence (cf. Refs. 13 and 14) indicate that no such spontaneous local moments exist, and hence the correlation effects may not be so dominant.

#### ACKNOWLEDGMENTS

The authors wish to acknowledge helpful discussions with S. H. Liu. They also wish to thank L. W. Bos and D. W. Lynch for communicating their results on the optical data in chromium in advance of publication.

#### APPENDIX

A typical oscillator-strength matrix element may

be written as

$$M_{kk'}(\vec{Q}) = \langle \psi_k(\vec{r}) | e^{-i\vec{Q} \cdot \vec{r}} | \psi_{k'}(\vec{r}) \rangle, \quad (A1)$$

where, as before,  $k$  includes both the Bloch wave vector  $\vec{k}$  and the band index, and  $\vec{Q} = \vec{q} + \vec{G}$ ,  $\vec{G}$  being a reciprocal-lattice vector. The wave function  $\psi_k(\vec{r})$  is expanded in the APW's as follows<sup>48</sup>:

$$\psi_k(\vec{r}) = \frac{1}{(\Omega)^{1/2}} \sum_{\vec{g}} a_{\vec{g}}^k \phi_{\vec{g}}^k(\vec{r}), \quad (A2)$$

where  $\Omega$  is the volume of the crystal,  $a_{\vec{g}}^k$  is the coefficient of expansion,  $\vec{g}$  is the reciprocal-lattice vector used in expansion, and  $\phi_{\vec{g}}^k(\vec{r})$  is an APW defined as

$$\phi_{\vec{g}}^k(\vec{r}) = e^{i\vec{k} \cdot \vec{r}}, \quad r > R \quad (A3)$$

$$\phi_{\vec{g}}^k(\vec{r}) = 4\pi e^{i\vec{k} \cdot \vec{R}_n}$$

$$\times \sum_{lm} \frac{i^l j_l(|\vec{k} + \vec{g}|R) Y_{lm}^*(\hat{k}_g) Y_{lm}(\hat{\rho}) R_l(k, \rho)}{R_l(k, R)}, \quad r < R \quad (A4)$$

where  $\vec{k}_g = \vec{k} + \vec{g}$ ,  $R$  is the radius of the APW sphere, and the distance  $\vec{r}$  from the origin is expressed as

$$\vec{r} = \vec{R}_n + \rho,$$

$\vec{R}_n$  being the lattice vector.  $R_l(k, \rho)$  denotes the radial wave function which, of course, depends only on the band energy and not the Bloch wave vector  $\vec{k}$ . All other symbols have their usual meaning. For  $r < R$ , (A2) may be written as

$$\begin{aligned} \Psi_k(r) &= \frac{1}{\Omega^{1/2}} \sum_{\vec{g}} a_{\vec{g}}^k 4\pi e^{i\vec{k} \cdot \vec{R}_n} \sum_{lm} i^l j_l(|\vec{k} + \vec{g}|R) \\ &\times Y_{lm}^*(\hat{k}_g) Y_{lm}(\hat{\rho}) \frac{R_l(k, \rho)}{R_l(k, R)} \\ &= 4\pi e^{i\vec{k} \cdot \vec{R}_n} \sum_{lm} i^l A_{lm}^k Y_{lm}(\hat{\rho}) \frac{R_l(k, \rho)}{R_l(k, R)}, \quad (A5) \end{aligned}$$

where

$$A_{lm}^k = \sum_{\vec{g}} a_{\vec{g}}^k j_l(|\vec{k} + \vec{g}|R) Y_{lm}^*(\hat{k}_g). \quad (A6)$$

Therefore,  $M_{kk'}(\vec{Q})$  may be written as

$$\begin{aligned} M_{kk'}(\vec{Q}) &= \sum_{\vec{g}, \vec{g}'} (a_{\vec{g}}^k)^* a_{\vec{g}'}^{k'} \sum_{\vec{K}} \delta(\vec{k} + \vec{g} - \vec{k}' - \vec{g}' + \vec{Q} - \vec{K}) \\ &\times [\delta_{\vec{K}, 0} - N V_0 G(KR)] + M_{kk'}^s(\vec{Q}), \quad (A7) \end{aligned}$$

where  $N$  is the number of atoms per unit volume,  $V_0$  is the volume of the APW sphere,  $\vec{K}$  is a reciprocal-lattice vector, and functions  $G(KR)$  and  $M_{kk'}^s(\vec{Q})$  are defined as

$$G(x) = 3(\sin x - x \cos x)/x^3 \quad (A8)$$

and

$$\begin{aligned} M_{kk'}^s(\vec{Q}) &= (4\pi)^2 N \sum_{ll'l''} \left| \frac{ll'l''}{kk'Q} \right| \sum_{mm'm''} \delta_{m', m+m''} \\ &\times (A_{lm}^k)^* A_{l'm''}^{k'} P_{l''}^{m''}(\cos\theta) e^{im''\phi} \end{aligned}$$

$$\times T(l'l'', mm'm'') \quad , \quad (A9)$$

where  $\vec{Q}$  is expressed as  $(Q, \theta, \varphi)$  in spherical coordinates, and

$$\left| \frac{l'l''}{kk'\vec{Q}} \right| = \int_0^R r^2 dr j_{l''}(Qr) \frac{R_l(k, r)}{R_l(k, R)} \frac{R_{l'}(k', r)}{R_{l'}(k', R)} \quad , \quad (A10)$$

$$T(l'l'', mm'm'') = (-i)^{l'-l''+l'''} (2l''+1) \left( \frac{2l+1}{2l'+1} \right)^{1/2} C(l'l'l'', 000) \\ \times C(l'l'l'', mm'm'') \left( \frac{(l''-|m''|)!}{(l''+|m''|)!} \right)^{1/2} \delta_{m', m+m''} \begin{cases} 1, & m'' \geq 0 \\ (-1)^{m''}, & m'' < 0 \end{cases} \quad (A11)$$

Here  $C(l'l'', mm'm'')$  is the Clebsch-Gordan coefficient.<sup>49</sup>  $T(l'l'', mm'm'')$  was calculated once and for all and stored.  $A_{lm}^k$  was evaluated for all values

of  $k$  in the irreducible  $\frac{1}{48}$ th of the Brillouin zone, and was stored with the coefficients  $a_k^k$  on magnetic tape.  $M_{kk'}(\vec{Q})$  is then easily evaluated.

<sup>†</sup> Work performed in the Ames Laboratory of the U.S. Atomic Energy Commission. Contribution No. 2686.

<sup>1</sup>C. G. Shull and M. K. Wilkinson, *Rev. Mod. Phys.* **25**, 100 (1953).

<sup>2</sup>A. W. Overhauser, *Phys. Rev. Letters* **4**, 462 (1960).

<sup>3</sup>A. W. Overhauser, *Phys. Rev.* **128**, 1437 (1962).

<sup>4</sup>G. Shirane and W. J. Takei, *J. Phys. Soc. Japan* Suppl. B **111**, **17**, 35 (1962).

<sup>5</sup>V. N. Bykov, V. S. Golovkin, N. V. Ageev, V. A. Levdik, and S. I. Vinogradov, *Dokl. Akad. Nauk SSSR* **128**, 1153 (1959) [*Soviet Phys. Doklady* **4**, 1070 (1960)].

<sup>6</sup>A. Arrott, S. A. Werner, and H. Kendrik, *Phys. Rev. Letters* **14**, 1022 (1965).

<sup>7</sup>W. C. Koehler, R. M. Moon, A. L. Trego, and A. R. Mackintosh, *Phys. Rev.* **151**, 405 (1966).

<sup>8</sup>P. A. Fedders and P. C. Martin, *Phys. Rev.* **143**, 245 (1966).

<sup>9</sup>A. Shibatani, K. Motizuki, and T. Nagamiya, *Phys. Rev.* **177**, 984 (1969).

<sup>10</sup>J. C. Kimball and L. M. Falicov, *Phys. Rev. Letters* **20**, 1164 (1968).

<sup>11</sup>J. C. Kimball, *Phys. Rev.* **183**, 533 (1969).

<sup>12</sup>S. Asano and J. Yamashita, *J. Phys. Soc. Japan* **23**, 714 (1967).

<sup>13</sup>C. Herring, in *Magnetism*, edited by G. T. Rado and H. Suhl (Academic, New York, 1966), Vol. 4.

<sup>14</sup>A. Arrott, in *Ref. 13*, Vol. 2 B.

<sup>15</sup>T. L. Loucks, *Phys. Rev.* **139**, A1181 (1965).

<sup>16</sup>F. Englert and M. M. Antonoff, *Physica* **30**, 429 (1964).

<sup>17</sup>H. Yamada and M. Shimizu, *J. Phys. Soc. Japan* **22**, 1404 (1967).

<sup>18</sup>H. Yamada and M. Shimizu, *J. Phys. Japan* **25**, 1001 (1968).

<sup>19</sup>J. B. Sokoloff, *Phys. Rev.* **180**, 613 (1969).

<sup>20</sup>J. B. Sokoloff, *Phys. Rev.* **185**, 770 (1969).

<sup>21</sup>J. B. Sokoloff, *Phys. Rev.* **185**, 783 (1969).

<sup>22</sup>J. Hubbard, *Proc. Roy. Soc. (London)* **A276**, 238 (1963).

<sup>23</sup>W. E. Evenson, G. S. Fleming, and S. H. Liu, *Phys. Rev.* **178**, 930 (1969).

<sup>24</sup>L. F. Mattheiss, *Phys. Rev.* **139**, A1893 (1965).

<sup>25</sup>P. Nozières and D. Pines, *Nuovo Cimento* **9**, 470 (1958).

<sup>26</sup>H. Ehrenreich and M. H. Cohen, *Phys. Rev.* **115**, 786 (1959).

<sup>27</sup>S. Adler, *Phys. Rev.* **126**, 413 (1962).

<sup>28</sup>N. Wiser, *Phys. Rev.* **129**, 62 (1963).

<sup>29</sup>M. Lax, *Lattice Dynamics* (Pergamon, New York, 1965), p. 184.

<sup>30</sup>R. Pick, M. H. Cohen, and R. M. Martin, in *Proceedings of IAEA Symposium on Inelastic Neutron Scattering, Copenhagen, Denmark, 1968* (International Atomic Energy Agency, Vienna, 1968), Vol. I, p. 119; *Phys. Rev. B* **1**, 910 (1970).

<sup>31</sup>W. M. Lomer, *Proc. Phys. Soc. (London)* **80**, 489 (1962).

<sup>32</sup>M. Asdente and J. Friedel, *Phys. Rev.* **124**, 384 (1961).

<sup>33</sup>D. Liberman, J. T. Waber, and D. T. Cromer, *Phys. Rev.* **137**, A27 (1965).

<sup>34</sup>L. W. Bos, Ph. D. thesis, Iowa State University, 1969 (unpublished); L. W. Bos and D. W. Lynch, *Phys. Rev. B* **2**, 4567 (1970).

<sup>35</sup>R. H. Pennington, *Introductory Computer Methods and Numerical Analysis* (MacMillan, New York, 1965).

<sup>36</sup>T. Clusius and P. Franzosini, *Gazz. Chim. Ital.* **93**, 221 (1963).

<sup>37</sup>T. M. Rice, A. S. Barker, Jr., B. I. Halperin, and D. B. McWhan, *J. Appl. Phys.* **40**, 1337 (1969).

<sup>38</sup>W. E. Evenson and S. H. Liu, *Phys. Rev.* **178**, 783 (1969).

<sup>39</sup>R. P. Gupta and S. K. Sinha, *J. Appl. Phys.* **41**, 915 (1970).

<sup>40</sup>A. S. Barker, Jr., B. I. Halperin, and T. M. Rice, *Phys. Rev. Letters* **20**, 384 (1968); also S. H. Liu (private communication).

<sup>41</sup>S. H. Liu, *Phys. Rev.* **139**, A1522 (1965).

<sup>42</sup>K. Kawasaki and H. Mori, *Progr. Theoret. Phys. (Kyoto)* **25**, 1043 (1961).

<sup>43</sup>L. J. Sham and J. M. Ziman, *Solid State Phys.* **15**, 221 (1963).

<sup>44</sup>S. K. Sinha, *Phys. Rev.* **177**, 1256 (1969).

<sup>45</sup>W. C. Cochran, *Proc. Roy. Soc. (London)* **A253**, 260 (1959).

<sup>46</sup>D. R. Penn, *Phys. Rev.* **142**, 350 (1966).

<sup>47</sup>M. K. Wilkinson, E. O. Wollan, W. C. Koehler, and J. W. Cable, *Phys. Rev.* **127**, 2080 (1962).

<sup>48</sup>T. L. Loucks, *Augmented Plane Wave Method* (Benjamin, New York, 1967).

<sup>49</sup>M. E. Rose, *Elementary Theory of Angular Momentum* (Wiley, New York, 1957).